An optimization of heat transfer of nanofluid flow in a helically coiled pipe using Taguchi method

Majid Mohammadi, Abazar Abadeh, Reza Nemati-Farouji & Mohammad Passandideh-Fard

Journal of Thermal Analysis and Calorimetry
An International Forum for Thermal Studies

ISSN 1388-6150
Volume 138
Number 2

J Therm Anal Calorim (2019)
138:1779-1792
DOI 10.1007/s10973-019-08167-y

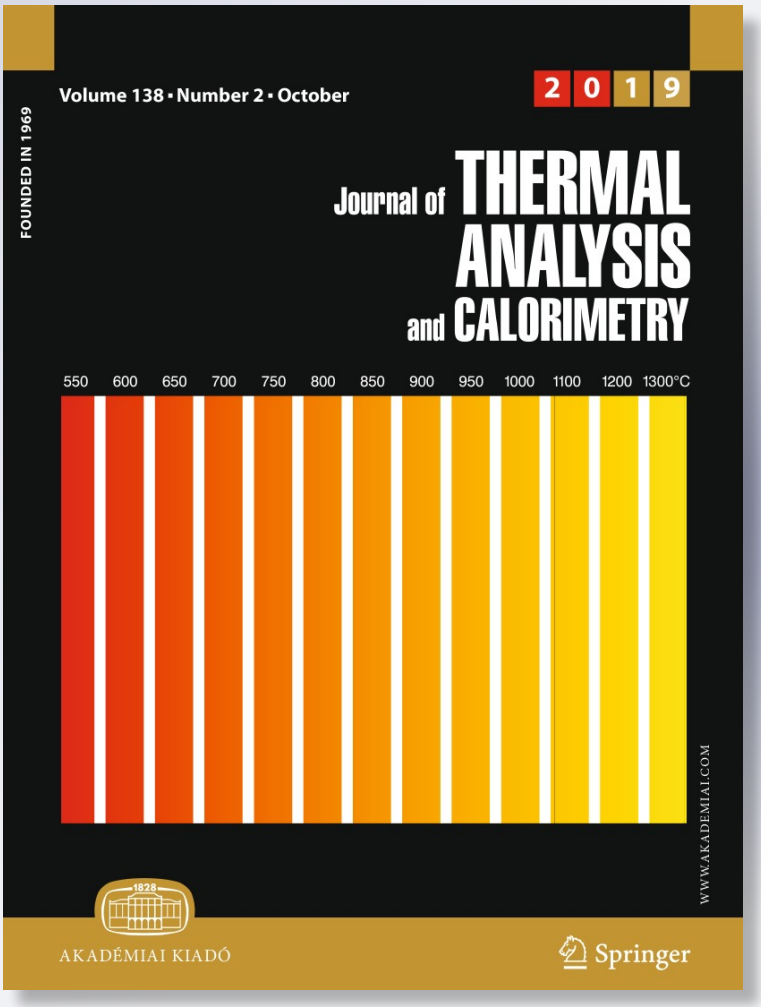

Springer

Journal of Thermal Analysis and Calorimetry (2019) 138:1779–1792
https://doi.org/10.1007/s10973-019-08167-y

An optimization of heat transfer of nanofluid flow in a helically coiled pipe using Taguchi method

Majid Mohammadi[1] · Abazar Abadeh[1] · Reza Nemati-Farouji[1] · Mohammad Passandideh-Fard[1]

Received: 20 November 2018 / Accepted: 4 March 2019 / Published online: 13 March 2019

Abstract

In this research, water–Fe_3O_4 nanofluid flow and heat transfer factors are optimized in a helically coiled pipe using Taguchi method. Numerical simulations using the ANSYS Fluent 18.2 are obtained first to provide the input data for the Taguchi method. Experiments are also performed to validate the results of the simulations. An experimental setup is constructed and initial experiments with water and water–Fe_3O_4 nanofluid are executed using various mass flow rates. A single-phase approach is employed as the numerical simulation model. The Taguchi method is selected as a test design method. Three different control factors (mass flow rate, coil curvature ratio and fluid type) with four levels are selected with the Taguchi method. An effective parameter, η, is defined to investigate the influence of different control parameters on heat transfer and fluid flow characteristics. Results show that mass flow rate is the most effective factor on η. Fluid type and the coil curvature ratio are next effective parameters, respectively. Through the course of this study, it is found that the best conditions to achieve the maximum η value are: mass flow rate value of 6.98 g s^{-1}, 1% vol. nanofluid as fluid type and coil curvature ratio of 0.048.

Keywords Helically coiled pipe · Nanofluid · Taguchi method

List of symbols

A	Area
C_p	Specific heat
d, R	Pipe diameter, pipe radius
D_c, a	Coil diameter, coil radius
f	Friction factor
$\bar{h}$	Average heat transfer coefficient
k	Conductivity
$\dot{m}$	Mass flow rate
Nu	Nusselt number
p	Coil pitch
q_s	Heat transfer rate
Re	Reynolds number
r	Radial position
T	Temperature
$\vec{V}$	Velocity vector
μ	Dynamic viscosity
υ	Kinematic viscosity
ρ	Density
φ	Nanoparticles volume fraction in the base fluid
ΔT_{lm}	Logarithmic temperature difference
ΔP	Pressure drop
η	Dimensionless parameter for optimization
δ	Uncertainty

Subscripts

bf	Base fluid
nf	Nanofluid
b, o	Bulk, outlet
b, i	Bulk, inlet
w	Distilled water
c	Coil
ave	Average

✉ Mohammad Passandideh-Fard
mpfard@um.ac.ir

Majid Mohammadi
mohammadi.ma@mail.um.ac.ir

Abazar Abadeh
abazar.abadeh@mail.um.ac.ir

Reza Nemati-Farouji
reza.nematifarouji@mail.um.ac.ir

[1] Department of Mechanical Engineering, Ferdowsi University of Mashhad, Mashhad, Iran

Introduction

Many today's industries use various energy saving methods as much as possible in their facilities due to the high prices of energy. Efforts have been made to enhance the heat transfer in heat exchangers, decrease the heat transfer duration and increase the energy utilization efficiency [1]. In general, two methods are available for heat transfer augmentation. Active methods are effective but could be extensively expensive. Mechanical mixing, rotation, vibration, electrostatic field and magnetic field are classified as active methods. On the other hand, passive methods are not as effective. However, they can be performed without further cost. Changing the geometry of the setup, modifying fluid property and altering flow regime from laminar to turbulent are the applicable examples of passive methods [1, 2].

One technique to increase the heat transfer rate is by changing the system geometry. It has been shown [3–5] that helical pipes employed in many industrial applications enhance the heat transfer due to the secondary flow induced by the centrifugal force. Hminic et al. [6] investigated heat transfer characteristics in double-tube helical heat exchangers by using nanofluids. They studied the effect of curvature and torsion ratio in helical pipes on the heat transfer. Manlapaz and Churchill [7] investigated the effect of torsion ratio in laminar flows in helical pipes. When the coil pitch was lower than the coil radius, they found the effect of torsion ratio to be negligible. Cioncolini and Santini [8] measured pressure drop for both laminar and turbulent flow regimes in different helical pipes. While the effect of curvature ratio was considerable, the effect of torsion ratio could be ignored.

Adding solid nanoparticles to a fluid modifies its thermophysical properties [3, 9–12]. Numerous studies have been performed in the literature to investigate the heat transfer increment by using nanofluids in other geometries [13, 14]. Akbaridoust et al. [15] experimentally and numerically investigated the convective heat transfer of nanofluid in helically coiled pipes at a constant wall temperature. Increasing the curvature ratio of the coiled pipe increased both the heat transfer coefficient and pressure drop. Moreover, they showed nearly 18 percent enhancement of the convective heat transfer coefficient in case of using water–CuO 0.2%, experimentally. Safari et al. [16] numerically studied turbulent forced convection flow of water and water–silver nanofluid in helical pipes using four-equation model. They reported that for higher Reynolds numbers the four-equation model shows a better agreement with experimental data in comparison with that of the homogenous model. The four-equation model, however, is more complex.

There are certain approaches to decrease the costs of experiments for which several investigations used the Taguchi method. Kotcioglu et al. [17] experimentally investigated the optimization of design parameters in a rectangular duct with plate-fins heat exchanger. In order to maximize the heat transfer and minimize the pressure drop in the heat exchanger, they determined optimal parameters. Hosseinzadeh et al. [18] optimized a nanofluid-based photovoltaic thermal system. They obtained the optimum operating conditions of their system based on the Taguchi analysis as: absorbed solar irradiation 1000 W m^{-2}, wind speed 1 m s^{-1}, ambient temperature 40 °C, coolant inlet temperature 20 °C, coolant mass flow rate 70 kg h^{-1} and ZnO nanoparticles mass fraction 12 mass%. Etghani et al. [19] numerically investigated and optimized heat transfer and exergy loss in a shell-and-helical tube heat exchanger. Their results indicate that the tube diameter and cold fluid flow rate have the most significant effect on heat transfer and exergy loss, respectively.

As mentioned before, heat transfer and fluid flow in helical coils are important in industrial applications. On the other hand, ferrofluid as a new generated fluid could affect the flow and heat transfer characteristics. But, studies on the factors that affect Fe_3O_4 nanofluid flow and heat transfer in helical coiled pipes at a constant wall temperature are rare in the literature. In this research, therefore, the effect of various working fluids, curvature ratio and the flow rate in a helical pipe is optimized using the Taguchi method. Furthermore, the effect of each parameter on each other and percentage effect for parameters are also measured. The optimization is performed to maximize the heat transfer rate and minimize the friction factor. Firstly, the experimental and numerical results are validated, and then the Taguchi tests are performed numerically.

Experimental and measurements

Experimental setup

Figure 1 displays the experimental apparatus from the previous experiment [20]. The cubic chamber that holds the coiled pipe is 250 × 350 × 300 mm and is well insulated on the outside. The chamber is equipped with a temperature controlling system by which any desired uniform temperature from ambient up to nearly 70 °C for the wall of the helical pipe could be achieved. The circular straight copper pipes with a 2 m length, 6.5 mm inner diameter and 0.7 mm thickness are used to fabricate the helically coiled pipes. Due to the high thermal conductivity of copper and small thickness of the pipe, the thermal resistance of the pipe wall could be ignored. Table 1 provides various coiled pipes with different curvature ratios used in this research. The pipe diameter is constant in all cases.

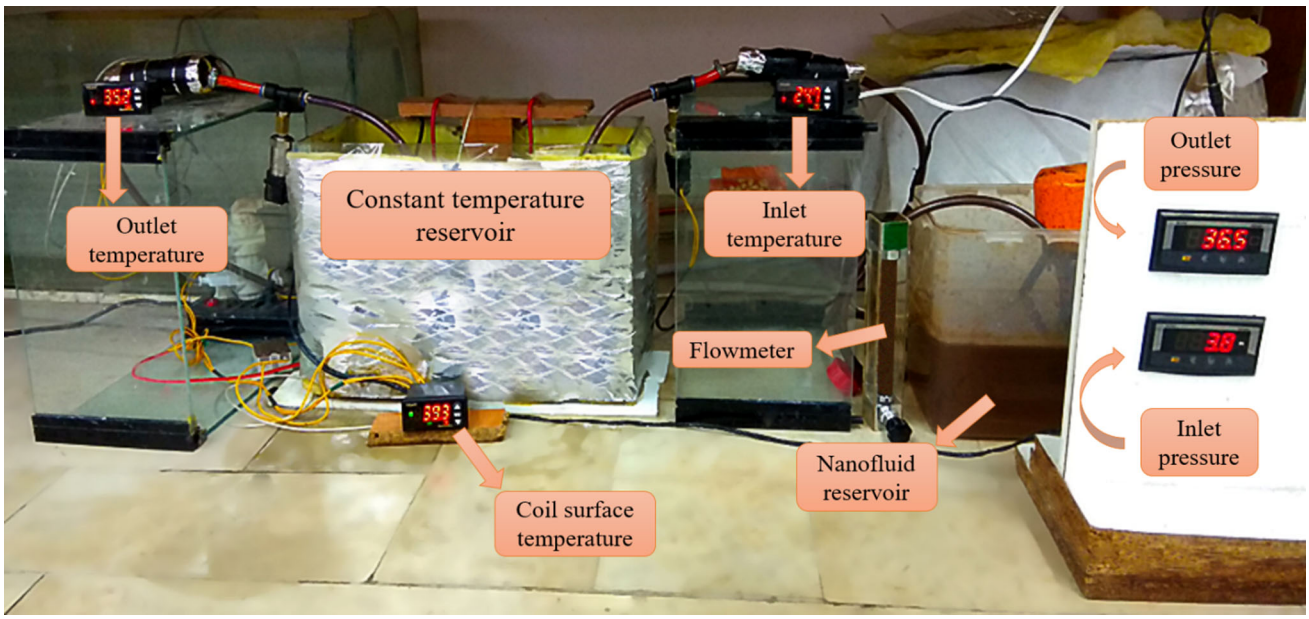

Fig. 1 A photograph of the experiment setup used in this study

Two high-precision pressure transmitters (BT 214 Pressure Transmitter, ATEK) are used to measure pressure drop between the inlet and outlet. The value of pressure is read by the transducer digital indicator. In order to measure the inlet and outlet temperatures, two calibrated RTD PT 100-type thermocouples with a precision of 0.1 °C are utilized. Each thermocouple is linked to a TC4Y indicator. The temperature controlling system is a kind of PID controller which is made of two heaters of 500 W, a TC4Y indicator, a RTD PT 100 thermocouple and a SSR (solid-state relay). In this research, the controller is set at a temperature of 40 °C. If the temperature is less than the desired temperature (40 °C), the TC4Y indicator sends a signal to the SSR to control the electric current such that the temperature remains constant at 40 °C.

A centrifugal pump drives the nanofluid from a reservoir tank through a calibrated flowmeter. The flowmeter sets the volumetric flow rate in the range of 10–60 L h^{-1} (LZB-10 glass tube rotameter). The heated nanofluid exiting the coiled pipe enters a cooling section equipped with a concentric counter flow heat exchanger. The whole experimental apparatus is displayed in Fig. 2.

Nanofluid preparation

In this research, all chemicals are used as received without any further treatment and are of analytical grade (chemical grade). In the experiments, twice-distilled water is selected as the base fluid and citric acid (CA) from Merck (Germany) as the surfactant. Fe_3O_4 nanoparticles are prepared from the US Research Nanomaterials, Inc., USA, with a purity of 98%, and their size is nearly 20–30 nm. To prepare nanofluid, a two-step method is used (a two-step preparation process is accomplished through mixing base fluid with the obtained nanoparticles) [21].

Figure 3 shows the production steps of the nanofluid. To prevent or decrease the agglomeration of Fe_3O_4 nanoparticles, they are grinded first by a mortar. Figures 4 and 5 show the TEM (transmission electron microscopy) images and DLS (dynamic light scattering) distribution of prepared nanoparticles, respectively. According to the DLS distribution, the mean diameter size of the nanoparticles is 21.22 nm. Next, Fe_3O_4 nanoparticles are added to the distilled water by one percent mass fraction and the mixture is stirred manually for at least 5 min [21].

Table 1 Characteristics of helically coiled pipes

Coil number	Coil diameter (mm) D	Total length (cm) L	Coil pitch (mm) p	δ
Coil 1	95	200	30	0.068
Coil 2	135	200	30	0.048
Coil 3	170	200	30	0.038
Coil 4	220	200	30	0.030

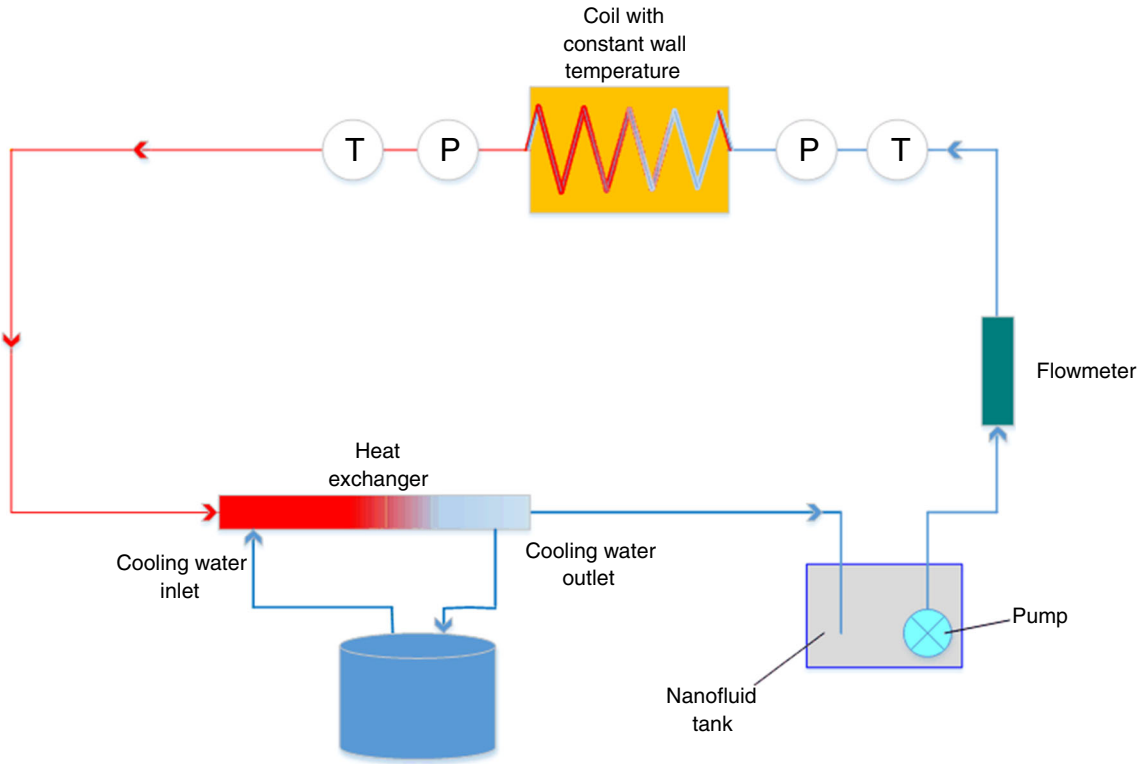

Fig. 2 A schematic of experimental setup [19]

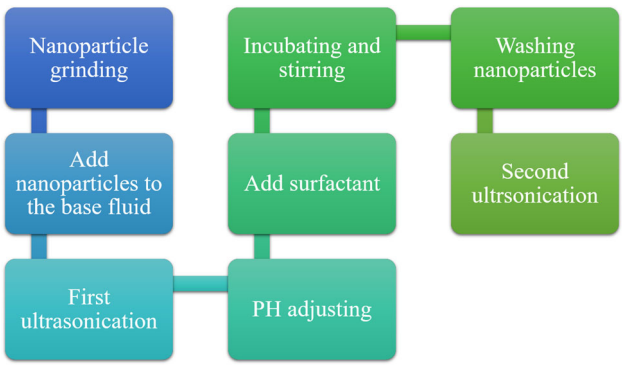

Fig. 3 A schematic of steps used for preparing nanofluids

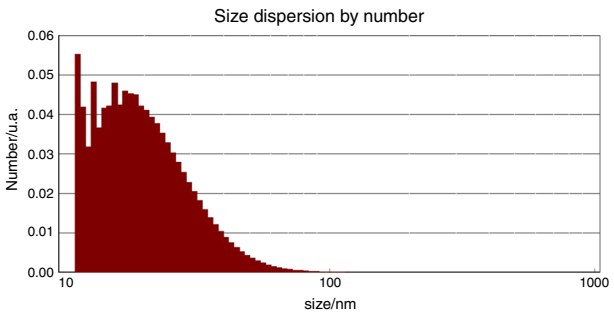

Fig. 4 A DLS report (particle size distribution) of nanoparticles [19]

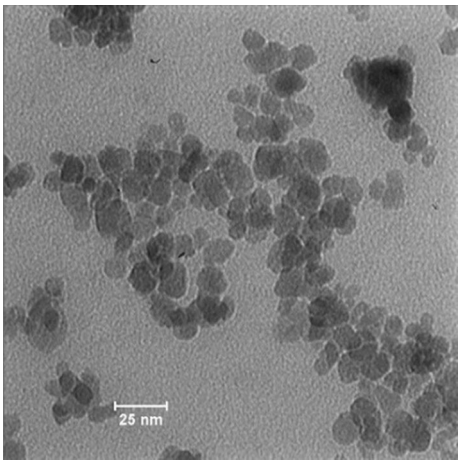

Fig. 5 A TEM image of Fe_3O_4 [19]

The prepared mixture is placed in the ultrasonic bath (Elma, Elmasonic, S60H, Germany) for an hour under a sonication with a frequency of 37 kHz, power of 400 watts and a temperature of 50 °C. The pH of the nanofluid is set at 11. Subsequently, the citric acid of 2 M is added to the mixture and stirred manually. The prepared mixture is incubated in a hot plate heater stirrer (Corning PC-420D, USA) with a speed of 600 rpm for 60 min which raises the suspension temperature up to 80 °C. Then, the mixture is washed several times with iridium magnets and distilled

water. The last step is to put the suspension in the ultrasonic bath for 20 min with a temperature set at 50 °C [21].

The zeta potential is used to investigate the final suspension (nanofluid) stability. The zeta potential is defined as the potential difference between the surface of nanoparticles immersed in a conducting liquid (here, water) and the bulk of the liquid. The magnitude of zeta potential is defined between 40 and 60 mV for a well-stabilized nanofluid [22]. As shown in Fig. 6, the zeta potential of the prepared nanofluid is 45.6.

Properties of nanofluid

With an assumption that the nanoparticles are uniformly dispersed within the base fluid, the effective physical properties of the nanofluid are evaluated using various relations available in the literature. Four main properties are conductivity, viscosity, density and heat capacity. Sundar et al. [23] presented the following relations for the properties of Fe_3O_4–water nanofluid:

$$k_{\mathrm{nf}} = k_{\mathrm{bf}}(1 + 0.5\varphi)^{0.1051} \tag{1}$$

$$\mu_{\mathrm{nf}} = \mu_{\mathrm{bf}}\left(1 + \frac{\varphi}{12.5}\right)^{6.356} \tag{2}$$

$$\rho_{\mathrm{nf}} = (1-\varphi)\rho_{\mathrm{W}} + \varphi\rho_{\mathrm{Fe_3O_4}}. \tag{3}$$

And for heat capacity the following relation is used [24]:

$$C_{\mathrm{p_{nf}}} = \frac{\varphi\rho_{\mathrm{Fe_3O_4}}C_{\mathrm{p_{Fe_3O_4}}} + (1-\varphi)\rho_{\mathrm{bf}}C_{\mathrm{p_{bf}}}}{\rho_{\mathrm{nf}}}. \tag{4}$$

Measurements

First, the amount of heat that the working fluid achieved from hot tube must be calculated in order to measure the average convective heat transfer coefficient:

$$q_{\mathrm{s}} = \dot{m}C_{\mathrm{p_{nf}}}(T_{\mathrm{b,o}} - T_{\mathrm{b,i}}), \tag{5}$$

where $\dot{m}$ is the mass flow rate, $C_{\mathrm{p_{nf}}}$ is the heat capacity of nanofluid, and $T_{\mathrm{b,i}}$ and $T_{\mathrm{b,o}}$ are the bulk temperature at the inlet and outlet of the constant wall temperature pipe, respectively.

To calculate the average convective heat transfer coefficient, q_{s} (amount of heat that working fluid achieves) must be substituted in the following relation:

$$q_{\mathrm{s}} = \bar{h}A\Delta T_{\mathrm{lm}} \tag{6}$$

$$\bar{h} = q_{\mathrm{s}}/A\Delta T_{\mathrm{lm}} \tag{7}$$

$$\Delta T_{\mathrm{lm}} = (\Delta T_2 - \Delta T_1)/\ln(\Delta T_2/\Delta T_1), \tag{8}$$

where ΔT_{lm} is the logarithmic mean temperature difference, $\bar{h}$ is the average convective heat transfer coefficient, $\Delta T_1 = T_{\mathrm{b,i}} - T_{\mathrm{s}}$, $\Delta T_2 = T_{\mathrm{b,o}} - T_{\mathrm{s}}$, and A is the lateral surface area of the pipe inside. Finally, the average Nusselt number and Reynolds number are calculated from:

$$Nu = \frac{\bar{h}d}{k} \tag{9}$$

$$Re = \frac{4\dot{m}}{\pi d\mu}, \tag{10}$$

where k is conductivity of the fluid. $\dot{m}$ is mass flow rate, d is the pipe inner diameter, and μ is dynamic viscosity of the fluid.

Equation 11 computes the friction factor of a fluid inside a pipe:

$$f = \frac{\Delta P}{\left(\frac{l}{d}\right)\left(\frac{\rho V^2}{2}\right)}, \tag{11}$$

where ΔP is pressure difference between inlet and outlet of coil, l is the length of pipe, d is the pipe diameter, ρ is the density of the nanofluid, and V is the velocity of the nanofluid in pipe.

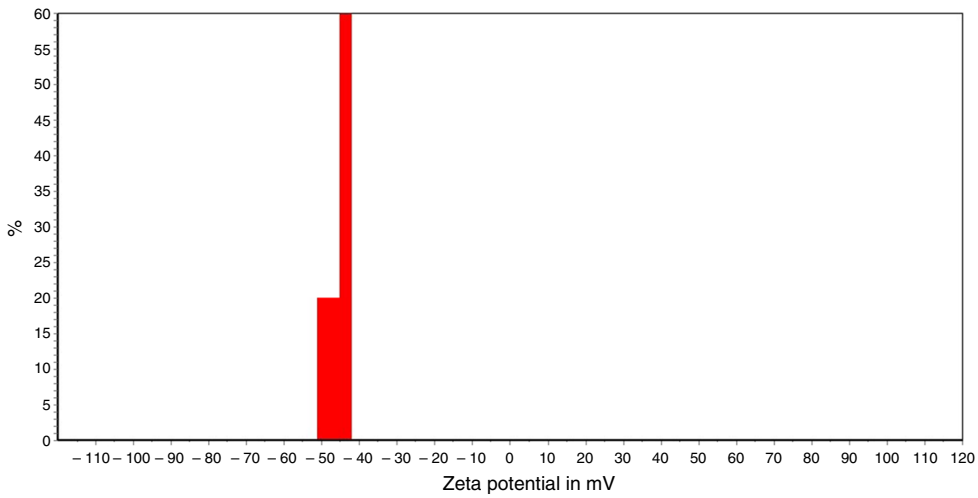

Fig. 6 A zeta potential report [20]

Table 2 Single- and two-phase models descriptions, assumptions, advantages and disadvantages

Model	Descriptions, assumptions	Advantages and disadvantages
Single-phase model	The slip between the based fluid and particle is negligible	Low computational costs
Homogenous	Uniform dispersion of the solid particles in the based fluid	Low accuracy comparing to experiments results
Thermal dispersion	Thermal and hydrodynamic equilibrium between the solid and liquid phase (Homo.)	Using novel models for thermophysical properties can reduce errors
Buongiorno	Raising the energy exchange rate in the nanofluid by the random motion of nanoparticles (Therm. dis.)	The heat transfer rate in geometrically simple problems can be estimated easily just by using accurate models for the nanofluid thermophysical properties
	Developing nonhomogeneous equilibrium model for transport equations in nanofluids (Buongiorno)	
Two-phase model	Considering two individual phases for solid nanoparticles and liquid based fluid	Longer simulation time and higher costs
Eulerian–Eulerian	Continuum interacting for based fluid and nanoparticles (Eulerian–Eulerian)	More complex model
Eulerian–Lagrangian	Continuum environment for based fluid and discrete phase for nanoparticles (Eulerian–Lagrangian)	More accurate results than the single-phase model

The curvature (δ) is presented by Cioncolini et al. [8]:

$$\delta = \frac{\pi^2 dD}{p^2 + \pi^2 D^2}. \tag{12}$$

In order to compare the performance of different coils with respect to both heat transfer and pressure drop, a dimensionless parameter usually used in the literature [3, 25] is defined as:

$$\eta = \frac{\bar{h}/\bar{h}_{\text{coil4}}}{\Delta P/\Delta P_{\text{coil4}}}. \tag{13}$$

Numerical simulation

Governing equations

In this study, the steady-state forced convection heat transfer through a helically coiled pipe using nanofluid is considered. The helical coil is assumed to remain at a constant temperature of T_s, and the fluid flow is assumed laminar.

Single- and two-phase are two general models for simulation of nanofluid flow and heat transfer. In single-phase models, the governing equations are solved only for the liquid phase. Homogenous, thermal dispersion and Buongiorno models are three categories of single-phase approaches. In the two-phase approaches, the based fluid and solid nanoparticles are modeled as two individual phases, with different velocity and temperature distributions. This method is divided into two general groups, Eulerian–Eulerian and Eulerian–Lagrangian models. Descriptions, assumptions, advantages and disadvantages of single- and two-phase models of nanofluid flow and heat transfer are presented in Table 2 [26].

In order to consider the interactions between the nanoparticles and the base fluid in simulation, two-phase model should be used. In this study, however, a single-phase model is employed. Since a large number of meshes need to be used in simulations, considering the nanoparticles/fluid interactions will lead to an increase in computational time and costs. Moreover, as the fluid flow is laminar (no complexity of turbulent flow), the use of a single-phase model is preferred in this study.

The governing equations for the conservation of mass, momentum and energy are solved in a Cartesian coordinate system:

$$\vec{\nabla}.\vec{V} = 0 \tag{14}$$

$$(\vec{V}.\vec{\nabla})\vec{V} = -\frac{\vec{\nabla}P}{\rho} + \upsilon\nabla^2\vec{V} \tag{15}$$

$$\rho C_p(\vec{V}.\vec{\nabla}T) = k\nabla^2 T, \tag{16}$$

where V is the velocity vector, P is the pressure, and T is the temperature.

The ANSYS©FLUENT (version R18.2) is used in this research. The SIMPLE algorithm is employed to couple pressure and momentum, and the second-order upwind scheme is utilized for the spatial discretization in all equations. The dependent variables (pressure, velocities and temperature) are under-relaxed by the factors of 0.3, 0.7 and 0.5 for P, V and T, respectively.

For boundary conditions, a constant mass flow rate with uniform temperature T_{in} is specified as the inlet boundary

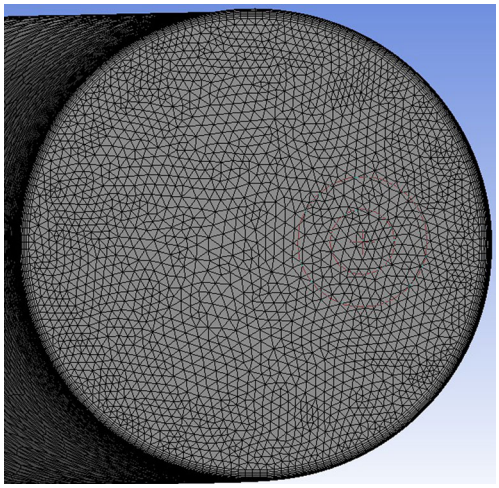

Fig. 7 Mesh in cross section of helically coiled pipe

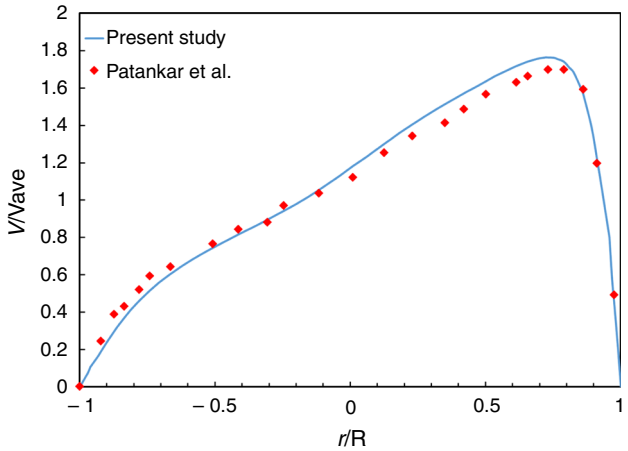

Fig. 9 Compression of this study velocity profile with Patankar et al. [27]

condition for the helically coiled pipe. The coil wall is assumed to be at a constant temperature T_s. The outlet boundary condition for the pipe is assumed to be the ambient.

A mesh refinement study is performed in this research where the size of the computational mesh is progressively increased until no significant changes in the simulation results are observed. Mesh in cross section of helically coiled pipe is presented in Fig. 7. Figure 8 shows the results of the mesh independency test for the average Nusselt number for a complex case with a maximum flow rate and a high volume concentration. As the figure indicates, the relative error of the average Nusselt number using a grid number of 700,000 (or greater) is less than

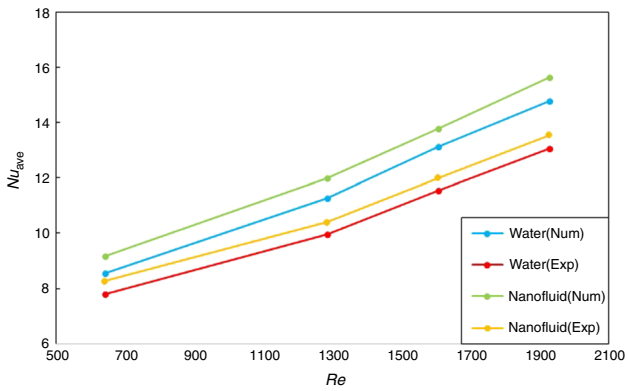

Fig. 10 Experimental and numerical results for variation of average Nusselt number versus different Reynolds numbers in Coil 2 (for distilled water and nanofluid 1 mass%)

Fig. 8 Mesh independency test: the effect of mesh size on average Nusselt number

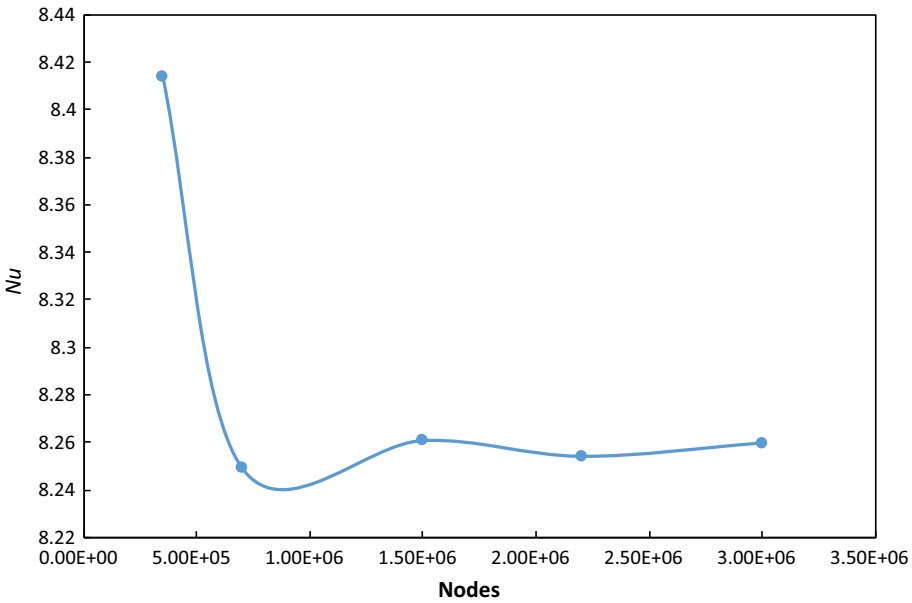

Table 3 Control factors and their corresponding levels

Factor	Level			
	1	2	3	4
Working fluid	Water	Nanofluid 0.2% vol.	Nanofluid 0.6% vol.	Nanofluid 1% vol.
Curvature ratio	0.068	0.048	0.038	0.030
Mass flow rate/g s^{-1}	2.79	4.19	5.59	6.98

Table 4 Tests plan of L_{16} (4^3) orthogonal array for the system

Test number	Mass flow rate	Curvature ratio	Fluid type
1	1	1	1
2	1	2	2
3	1	3	3
4	1	4	4
5	2	1	2
6	2	2	1
7	2	3	4
8	2	4	3
9	3	1	3
10	3	2	4
11	3	3	1
12	3	4	2
13	4	1	4
14	4	2	3
15	4	3	2
16	4	4	1

0.14% compared to the case with a grid number of 1,500,000.

Validation of numerical results

Validation of the present study with Patankar et al. [27] is presented in Fig. 9 for Dean number of 372. As it clear in this figure, the result shows a good agreement with the previous study. Numerical results are also validated using a single-phase homogenous approach. Figure 10 shows a comparison between the experimental results of the designed apparatus and the numerical results for pure water and nanofluid in Coil 2. The figure shows that using a single-phase fluid model, the numerical results well predict the experimental measurements with an error of nearly 14%. This is an indication of the validity of the single-phase model for the system under consideration.

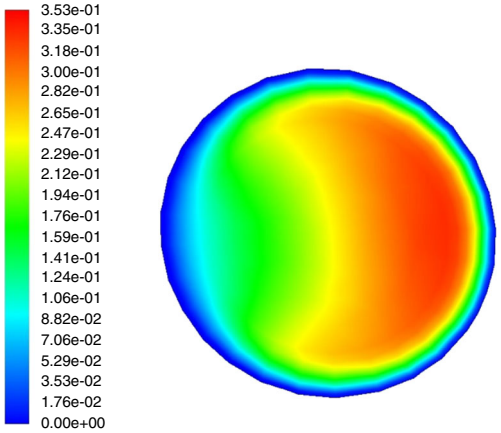

Fig. 11 Velocity distribution in a coil cross section area (Coil 2)

Taguchi method theory

To reduce the cost of experiments, several approaches are presented. Lui et al. [28] investigated parameter study of the injection configuration in a zero boil-off hydrogen storage tank using orthogonal test design. They optimize the structural parameter of the interior injection configuration to analyze the fluid flow and heat transfer inside the storage tank and improve the performance. Taguchi method is one of the powerful design and optimization methods, which is employed to determine the values of control factors discretely to reach the optimal value of objectives [29]. This method is also employed in this paper, which is developed by Taguchi to improve the process or product quality by statistical concepts and so is called the Taguchi method. Due to its wide range of applications, this method has been used extensively in engineering analyses. It has been proved that the method can be very effective, provided that proper considerations are taken into account [30]. The Taguchi is an experimental optimization method that uses the standard orthogonal arrays that form the matrix of experiments. It helps to get a maximum value of information from a minimum number of tests and, subsequently, to find the best level of each factor [31]. This method is an optimal parametric design of experimental tool, which first chooses several effective parameters of relative characteristics and puts them into an appropriate plan table with several levels for each factor [32]. Some of

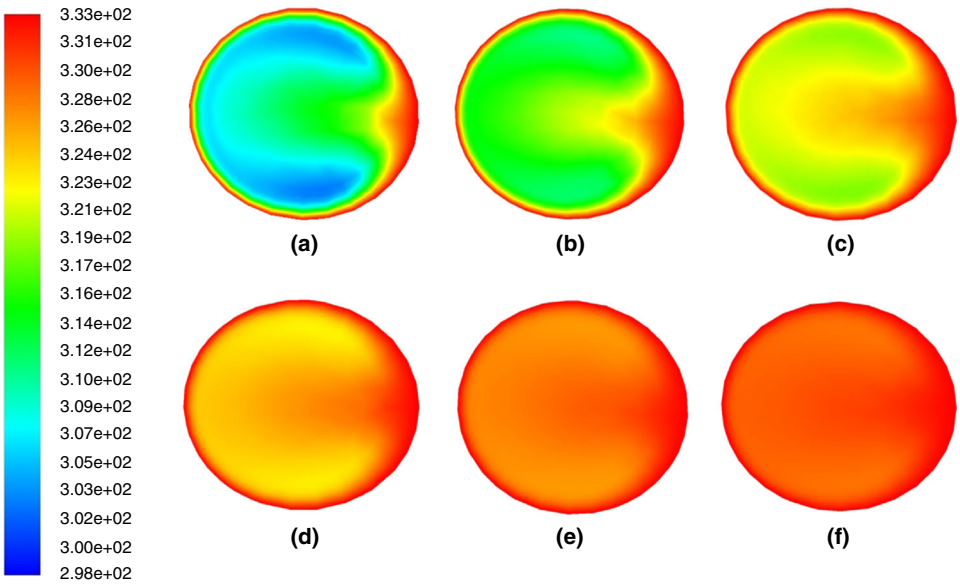

Fig. 12 Temperature distribution for six different cross sections (Coil 2)

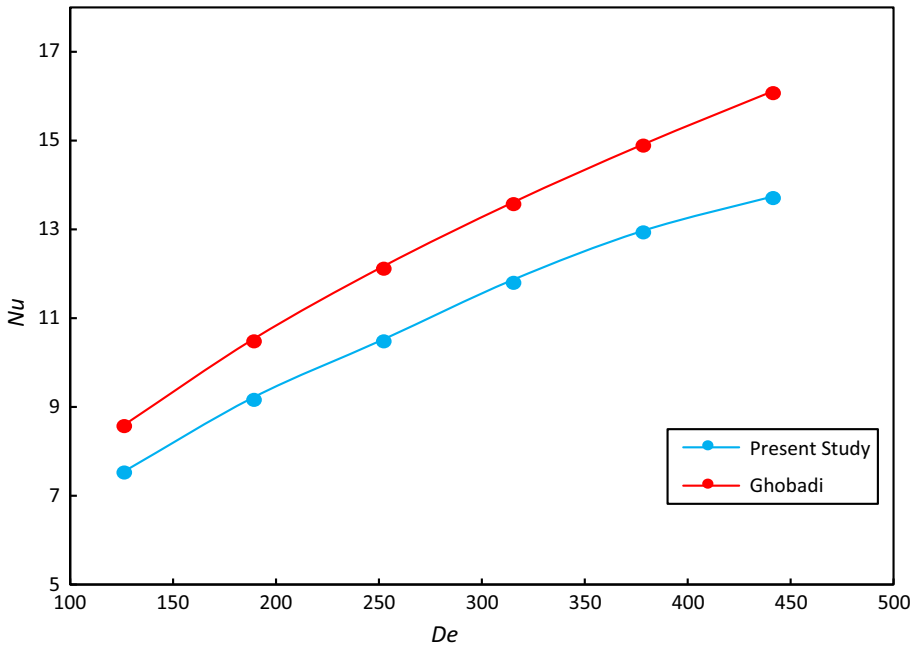

Fig. 13 Ghobadi correlation versus present study

advantages of the Taguchi method over the other conventional experimental methods are: reducing the experimental cost, minimizing the variability around the target when bringing the performance value to the target value and reproducing optimum working conditions determined from the laboratory study in real applications [17].

In this method, according to the existing system, the number of factors and levels is identified. First, the appropriate orthogonal array (OA) is selected based on the number of control factors and levels. Next, the optimum number of experiments is determined. The minimum number of experiments needed in the Taguchi optimization technique can be determined as:

$$N_{\text{Taguchi}} = 1 + NV(J - 1), \tag{17}$$

where N_{Taguchi}, J and NV are the number of experiments, the level and given number of the control factors, respectively [17].

To calculate the responses in data analyzing, signal-to-noise (SN) ratios are used. Three types of performance characteristics are applied in the analysis: larger-is-better, smaller-is-better and nominal-is-better [17]. The signal-to-noise analysis by two performances of larger-is-better and smaller-is-better is defined as follows:

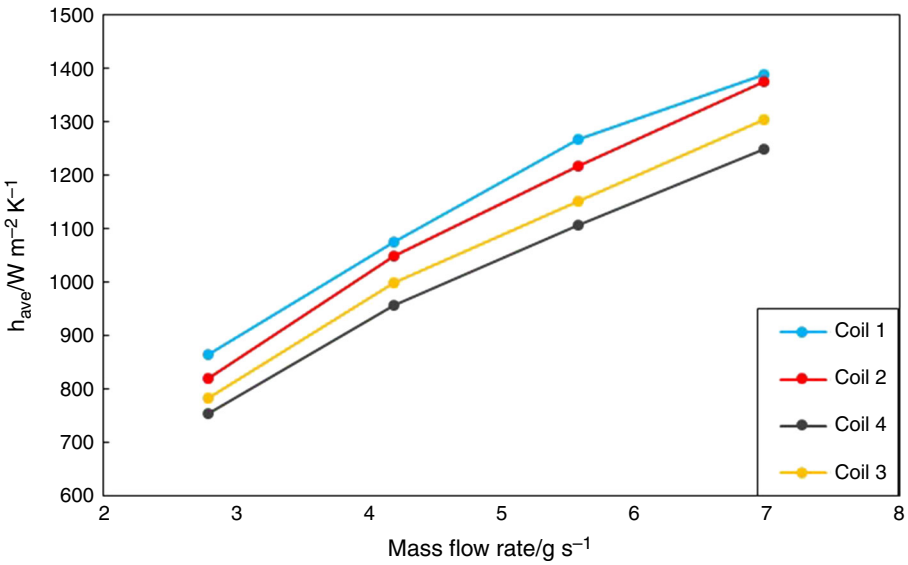

Fig. 14 Variation of the convective heat transfer versus mass flow rate for nanofluid (experimental)

$$\mathrm{SN} = -10\log_{10}\left(\frac{1}{n}\sum_{i=1}^{n}\frac{1}{y_i^2}\right) \tag{18}$$

$$\mathrm{SN} = -10\log_{10}\left(\frac{1}{n}\sum_{i=1}^{n}y_i^2\right), \tag{19}$$

where y_i is a quality measurement and n is the total number of the experiments.

After performing the experiments, by using the signal-to-noise ratio, the results are analyzed. To obtain the contribution of individual factor in the test, the ANOVA (analyze of variance) is applied.

Selection of the effective factors on η parameter

This study considers three design parameters as control factors. These factors are mass flow rate, coil curvature ratio and working fluid type. The levels of each factor are depicted in Table 3 where four levels are selected for each control factor. It is argued that the Taguchi method optimizes the average Nusselt number and friction factor by choosing the optimal control factors discretely.

Design of experiments

In this paper, design of experiments is accomplished by the Taguchi method. As mentioned in Table 3, there are three factors with four levels (mass flow rate, coil curvature ratio and working fluid type). Using the Minitab software and choosing the Taguchi as the experimental designing method, 16 experiments are designed as given in Table 4. The result of each test is evaluated based on the value of η parameter. Obviously, for a higher η value, the coil will have a better performance; therefore, the criterion of "larger-is-better" is selected. The Taguchi tests are performed numerically.

Results and discussion

Initial results

The experiments are performed in a laminar flow with four different Reynolds numbers ($600 < Re < 2000$). Coils configurations are given in Table 1. Then, the temperature distribution at six different distances from inlet for coil with curvature ratio of 0.048 and mass flow rate of 5.59 kg s^{-1} is investigated. The secondary flow due to centrifugal force has significantly affected the temperature and velocity distribution in each cross section area of the coil. The velocity distribution for an arbitrary cross section is shown in Fig. 11. Raising the velocity of the fluid leads to decrease in temperature in each computational cell. This happened because when the velocity increases, convective heat transfer enhances, so the fluid temperature decreases. This phenomenon is investigated in Fig. 12. The figure shows the variation of the temperature in six different cross sections with the distance of πD/2 between each two continuous cross sections. D is the coil diameter.

In Fig. 13, the experimental results for Coil 3 in six different Dean numbers are compared with the presented correlation by Ghobadi and Muzychka [33]. They studied fully developed heat transfer in mini-scale coiled tubing for constant wall temperature.

$$Nu = 0.91375\sqrt{De}Pr^{-0.1}. \tag{20}$$

The results showed that the present study is performed well.

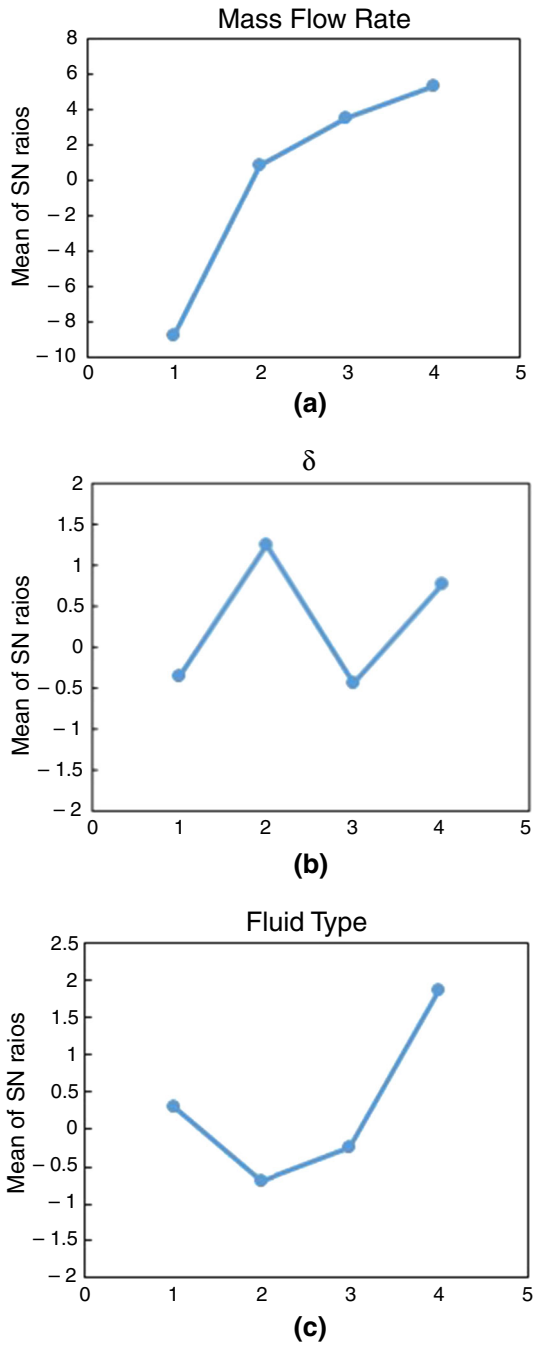

Fig. 15 Effects of different control factors on η parameter

In the present work, the important factors that affect heat transfer rate and pressure drop in laminar, incompressible, steady-state viscous flow in the helically coiled pipes at a constant wall temperature are optimized by the Taguchi method. The variation of the convective heat transfer vs. mass flow rate for the nanofluid is shown in Fig. 14. Different particle volume concentrations are considered inside different helical pipes.

Table 5 Mean effects of the factors in each level

Factors	Level 1	Level 2	Level 3	Level 4
Working fluid	1.25	1.06	1.16	1.44
Curvature ratio	1.20	1.36	1.11	1.24
Mass flow rate/g s^{-1}	0.37	1.13	1.53	1.87

Optimization results (Taguchi)

The effect of each factor is indicated in Fig. 15. The η parameter is increased by increasing the mass flow rate as shown in Fig. 15a. Moreover, the curve slope in this figure is decreased which means that the influence of flow rate increment is reduced for higher mass flow rates.

The heat transfer coefficient is enhanced by decreasing the coil curvature ratio. This is because a smaller curvature ratio increases the centrifugal force. But increasing the curvature ratio also increases the pressure drop that is not desirable. Based on the Taguchi tests, using the coil curvature ratio the η value cannot be determined. As shown in this figure, for Coil 2 the value of η is maximum.

The last factor is the working fluid type. Adding nanoparticle enhances the average Nusselt number but increases the friction factor at the same time. Thus, the η value in each case must be examined because similar to the curvature ratio, the variation of eta does not follow a special trend. As shown in Fig. 15b, the forth fluid (1% vol. nanofluid) has the largest η value. Next, water has a larger eta in comparison with nanofluid 0.2% and 0.6% vol. This means that adding nanoparticles to the base fluid is not always a good way to have an optimum coil. Hence, for an optimum coil (with maximum heat transfer rate and minimum pressure drop) the operating conditions are: 6.98 g s^{-1} mass flow rate, curvature ratio of $\delta = 0.048$ (Coil 2) and nanofluid 1% vol. as the working fluid.

Analysis of the factors effects

The effect of each factor on η parameter is an important point which must be determined. In order to achieve this purpose, the Taguchi uses an analysis of variance (ANOVA). Table 5 shows the results of ANOVA of the test factors. This table indicates that the contribution of the working fluid type, the coil curvature ratio and the mass flow rate on η value is 31.4, 31.1 and 37.4, respectively. According to the standards presented by Taguchi [34], if the amount of error measured from ANOVA is less than 15 percent, the results are reliable and valid; otherwise, the tests must be performed again with a higher accuracy. As given in Table 6, the measured error from ANOVA is

Table 6 Variance and the percentage effect of each factor

Factors	Variance	Squares summation	Percentage effect
Working fluid	0.381	6.102	31.41
Curvature ratio	0.244	6.054	31.16
Mass flow rate/g s^{-1}	1.500	7.272	37.43
Error	0.002	0.007	–

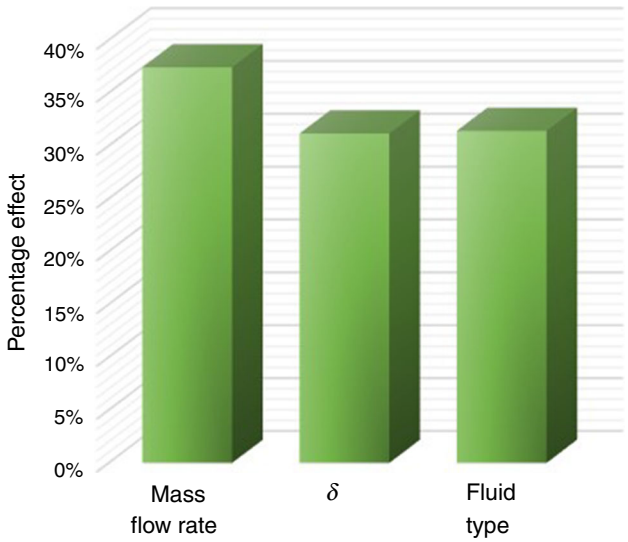

Fig. 16 Percentage effect of each factor

small and, therefore, the results are reliable. The percentage effect of the factors is also presented in Fig. 16 where it is seen that the mass flow rate is the most effective factor on η value.

Conclusions

According to the experimental and numerical investigations performed in this study, the following results are concluded:

- For a nanofluid (Fe_3O_4–water 1 mass%) in laminar flow, a single-phase model in the simulations results in a good comparison with the measurements and with nearly 15% error.
- The effective factors in the Taguchi method optimization are considered to be working fluid type, coil curvature ratio and mass flow rate. For each factor, four levels were considered in this study. The Taguchi method resulted in an optimized case with these values for the effective factors: 6.98 g s^{-1} mass flow rate, 0.048 curvature ratio (Coil 2) and nanofluid 1% vol.
- In order to determine how the factors affect η, an analysis of variance (ANOVA) is performed. The results indicate that the percentage effect of the factors is 31.4, 31.1 and 37.4, respectively.

Appendix: Uncertainty analysis

In order to investigate the reliability of the measurements, an uncertainty analysis is performed for the experimental data [35]. The values of uncertainties estimated with different instruments are given in Table 7. The maximum possible error for the parameters involved in the analysis are estimated and summarized. For example, for calculating the absolute uncertainty of Nusselt number, the following relation is employed [36]:

Table 7 Measurement devices, their information and uncertainty

Number	Instrument	Range	Measured parameter	Accuracy	Min and Max measurable value	Relative uncertainty
1	PTD PT 100 thermocouple	0–200 °C	Inlet and outlet temperature	0.1	24.5–41	0.244
2	Pressure transducer	0–100 mbar	Inlet and outlet pressure	0.1	1.5–42	0.238
3	Flowmeter	0–70 L h^{-1}	Fluid flow rate	1	10–60	1.667
4	Geometry dimensions	1–20 mm	Pipe diameter and thickness	0.1	1–20	0.5
5	Physical properties	–	Conductivity, density, heat capacity, viscosity	–	–	0.1

Table 8 Uncertainty of different parameters

Parameter	Relative uncertainty
ΔT_{lm}	0.422
h	1.676
Re	1.670
Nu	1.708

$$\delta Nu = \sqrt{\left(\frac{\partial Nu}{\partial h}\delta h\right)^2 + \left(\frac{\partial Nu}{\partial D}\delta D\right)^2 + \left(\frac{\partial Nu}{\partial K}\delta K\right)^2}, \quad (21)$$

and for the relative uncertainty:

$$\frac{\delta Nu}{Nu} = \sqrt{\left(\frac{\delta h}{h}\right)^2 + \left(\frac{\delta D}{D}\right)^2 + \left(\frac{\delta K}{K}\right)^2}. \quad (22)$$

Similarly, for other parameters, we have:

$$\frac{\delta \Delta T_{lm}}{\Delta T_{lm}} = \sqrt{\left(\frac{\delta T_{b,i}}{T_{b,i}}\right)^2 + \left(\frac{\delta T_{b,o}}{T_{b,o}}\right)^2 + \left(\frac{\delta T_s}{T_s}\right)^2} \quad (23)$$

$$\frac{\delta h}{h} = \sqrt{\left(\frac{\delta q_s}{q_s}\right)^2 + \left(\frac{\delta \Delta T_{lm}}{\Delta T_{lm}}\right)^2 + \left(\frac{\delta A}{A}\right)^2} \quad (24)$$

$$\frac{\delta Re}{Re} = \sqrt{\left(\frac{\delta \upsilon}{\upsilon}\right)^2 + \left(\frac{\delta d}{d}\right)^2 + \left(\frac{\delta v}{v}\right)^2}. \quad (25)$$

Table 8 presents the relative uncertainty of various parameters used in this research.

References

1. Huminic G, Huminic A. Application of nanofluids in heat exchangers: a review. Renew Sustain Energy Rev. 2012;16(8):5625–38.
2. Wen D, Lin G, Vafaei S, Zhang K. Review of nanofluids for heat transfer applications. Particuology. 2009;7(2):141–50.
3. Rakhsha M, Akbaridoust F, Abbassi A, Majid S-A. Experimental and numerical investigations of turbulent forced convection flow of nano-fluid in helical coiled tubes at constant surface temperature. Powder Technol. 2015;283:178–89.
4. Suresh S, Chandrasekar M, Selvakumar P. Experimental studies on heat transfer and friction factor characteristics of CuO/water nanofluid under laminar flow in a helically dimpled tube. Heat Mass Transf. 2012;48(4):683–94.
5. Xin R, Ebadian M. The effects of Prandtl numbers on local and average convective heat transfer characteristics in helical pipes. J Heat Transf. 1997;119(3):467–73.
6. Huminic G, Huminic A. Heat transfer characteristics in double tube helical heat exchangers using nanofluids. Int J Heat Mass Transf. 2011;54(19–20):4280–7.
7. Manlapaz RL, Churchill SW. Fully developed laminar flow in a helically coiled tube of finite pitch. Chem Eng Commun. 1980;7(1–3):57–78.
8. Cioncolini A, Santini L. An experimental investigation regarding the laminar to turbulent flow transition in helically coiled pipes. Exp Therm Fluid Sci. 2006;30(4):367–80.
9. Zhu H, Han D, Meng Z, Wu D, Zhang C. Preparation and thermal conductivity of CuO nanofluid via a wet chemical method. Nanoscale Res Lett. 2011;6(1):181.
10. Yu W, France DM, Routbort JL, Choi SU. Review and comparison of nanofluid thermal conductivity and heat transfer enhancements. Heat Transf Eng. 2008;29(5):432–60.
11. Pang C, Jung J-Y, Kang YT. Thermal conductivity enhancement of Al_2O_3 nanofluids based on the mixtures of aqueous NaCl solution and CH_3OH. Int J Heat Mass Transf. 2013;56(1–2):94–100.
12. A.I.A. AL-Musawi, A. Taheri, A. Farzanehnia, M. Sardarabadi, M. Passandideh-Fard. Numerical study of the effects of nanofluids and phase-change materials in photovoltaic thermal (PVT) systems. J Therm Anal Calorim. 2018. https://doi.org/10.1007/s10973-018-7972-6.
13. Goharkhah M, Ashjaee M, Shahabadi M. Experimental investigation on convective heat transfer and hydrodynamic characteristics of magnetite nanofluid under the influence of an alternating magnetic field. Int J Therm Sci. 2016;99:113–24.
14. Zonouzi SA, et al. Experimental investigation of the flow and heat transfer of magnetic nanofluid in a vertical tube in the presence of magnetic quadrupole field. Exp Therm Fluid Sci. 2018;91:155–65.
15. Akbaridoust F, Rakhsha M, Abbassi A, Saffar-Avval M. Experimental and numerical investigation of nanofluid heat transfer in helically coiled tubes at constant wall temperature using dispersion model. Int J Heat Mass Transf. 2013;58(1–2):480–91.
16. A. Safari, M. Saffar-Avval, E. Amani, Numerical investigation of turbulent forced convection flow of nano fluid in curved and helical pipe using four-equation model. Powder Technol. 2018;328:47–53.
17. Kotcioglu I, Cansiz A, Khalaji MN. Experimental investigation for optimization of design parameters in a rectangular duct with plate-fins heat exchanger by Taguchi method. Appl Therm Eng. 2013;50(1):604–13.
18. Hosseinzadeh M, Salari A, Sardarabadi M, Passandideh-Fard M. Optimization and parametric analysis of a nanofluid based photovoltaic thermal system: 3D numerical model with experimental validation. Energy Convers Manag. 2018;160:93–108.
19. Etghani MM, Baboli SAH. Numerical investigation and optimization of heat transfer and exergy loss in shell and helical tube heat exchanger. Appl Therm Eng. 2017;121:294–301.
20. A. Abadeh, M. Mohammadi, M. Passandideh-Fard. Experimental investigation on heat transfer enhancement for a ferrofluid in a helically coiled pipe under constant magnetic field. J Therm Anal Calorim. 2019;135(2):1069–79.
21. A. Abadeh, M. Passandideh-Fard, M.J. Maghrebi, M. Mohammadi. Stability and magnetization of Fe_3O_4/water nanofluid preparation characteristics using Taguchi method. J Therm Anal Calorim. 2019;135(2):1323–34.
22. J. Mohamoud, S. Tejvir. Critical review on nanofluids: preparation characterization and applications. J Nanomater.
23. Sundar LS, Singh MK, Sousa AC. Investigation of thermal conductivity and viscosity of Fe_3O_4 nanofluid for heat transfer applications. Int. Commun. Heat Mass Transf. 2013;44:7–14.
24. Maadi SR, Kolahan A, Passandideh-Fard M, Sardarabadi M, Moloudi R. Characterization of PVT systems equipped with nanofluids-based collector from entropy generation. Energy Convers Manag. 2017;150:515–31.
25. Akhavan-Behabadi M, Pakdaman MF, Ghazvini M. Experimental investigation on the convective heat transfer of nanofluid flow inside vertical helically coiled tubes under uniform wall

temperature condition. Int Commun Heat Mass Transf. 2012;39(4):556–64.
26. Mahian O, et al. Recent advances in modeling and simulation of nanofluid flows-Part I: fundamentals and theory. Phys Rep. 2019;790:1–48.
27. Patankar SV, Pratap VS, Spalding DB. Prediction of laminar flow and heat transfer in helically coiled pipes. J Fluid Mech. 1974;62(3):117–29.
28. Liu Y, Wu R, Yang P, Wang T, Liu H, Wang L. Parameter study of the injection configuration in a zero boil-off hydrogen storage tank using orthogonal test design. Appl Therm Eng. 2016;109:283–94.
29. Wang H, Liu Y-W, Yang P, Wu R-J, He Y-L. Parametric study and optimization of H-type finned tube heat exchangers using Taguchi method. Appl Therm Eng. 2016;103:128–38.
30. Li Q, Xuan Y, Wang J. Experimental investigations on transport properties of magnetic fluids. Exp Therm Fluid Sci. 2005;30(2):109–16.
31. Bica D, Vekas L, Raşa M. Preparation and magnetic properties of concentrated magnetic fluids on alcohol and water carrier liquids. J Magn Magn Mater. 2002;252:10–2.
32. Wang X, Zhang C, Wang X, Gu H. The study on magnetite particles coated with bilayer surfactants. Appl Surf Sci. 2007;253(18):7516–21.
33. M. Ghobadi, Y.S. Muzychka. Fully developed heat transfer in mini scale coiled tubing for constant wall temperature. In: ASME 2013 International Mechanical Engineering Congress and Exposition. American Society of Mechanical Engineers; 2013. p. V08CT09A048.
34. R.K. Roy, A primer on the Taguchi method. Society of Manufacturing Engineers; 2010.
35. Farzanehnia A, Khatibi M, Sardarabadi M, Passandideh-Fard M. Experimental investigation of multiwall carbon nanotube/paraffin based heat sink for electronic device thermal management. Energy Convers Manag. 2019;179:314–25.
36. Sundar LS, Naik M, Sharma K, Singh M, Reddy TCS. Experimental investigation of forced convection heat transfer and friction factor in a tube with Fe_3O_4 magnetic nanofluid. Exp Therm Fluid Sci. 2012;37:65–71.